Supplementary Material on "Crack wave resonances within the basal water layer"

Dominik GRÄFF,[1] Fabian WALTER,[1], Bradley P. LIPOVSKY[2]

[1] *Laboratory of Hydraulics, Hydrology and Glaciology, ETH Zurich, Switzerland*
[2] *Department of Earth and Planetary Science, Harvard University, Cambridge MA, USA*
Correspondence: Dominik Gräff <graeff@vaw.baug.ethz.ch>

INSTRUMENTATION

Pressure Sensor in 2017

We operate one piezoresistive pressure sensor model PAA-26W from Keller AG für Druckmesstechnik at the bed of Rhonegletscher with following specifications:

operational pressures:	0.7 - 41 bar abs
linearity:	0.5 % full scale
corner frequency:	1.2 kHz
output signal:	0.4 - 20 mA

We read out the electric potential via a 51 Ohm resistor with a Nanometrics Centaur digitizer with 26 dB gain, sampled at 1000 Hz. To convert the counts of the digitizer to Pa, we apply the following conversion:

$$p\ (\mathrm{Pa}) = \left[\frac{\mathrm{cnts}}{1.62 \cdot 10^5\ \mathrm{cnts/bar}} - 9.39\,\mathrm{bar}\right] \times 10^5\ \mathrm{Pa/bar} - 744\,\mathrm{hPa}$$

where 744 hPa is the air pressure at 2300 m a.s.l. calculated with a simple exponential barometric pressure following $p(h) = h_0\ exp\,(-h/8435\,m)$ assuming $h_0 = 1000$ hPa.

The times of deployment at the glacier bed are (UTC):
2017-08-17 15:54:00 - 2017-08-18 11:17:00
2017-08-21 09:07:00 - 2017-08-21 10:59:00
2017-08-21 12:12:00 - 2017-08-21 15:22:00
2017-08-21 16:09:00 - 2017-08-22 17:21:00
2017-08-23 15:22:00 - 2017-08-23 16:48:00
2017-08-24 09:04:00 - 2017-08-24 14:29:00

Pressure Sensors in 2018

Similar to 2017, but with 4 sensors with 0.2 % full scale linearity. The signal is read out via a 5 Ohm resistor with a Nanometrics High-Gain Centaur digitizer with 44 dB gain sampled at 2000 Hz. Figure 1 shows a map of borehole locations in 2018.

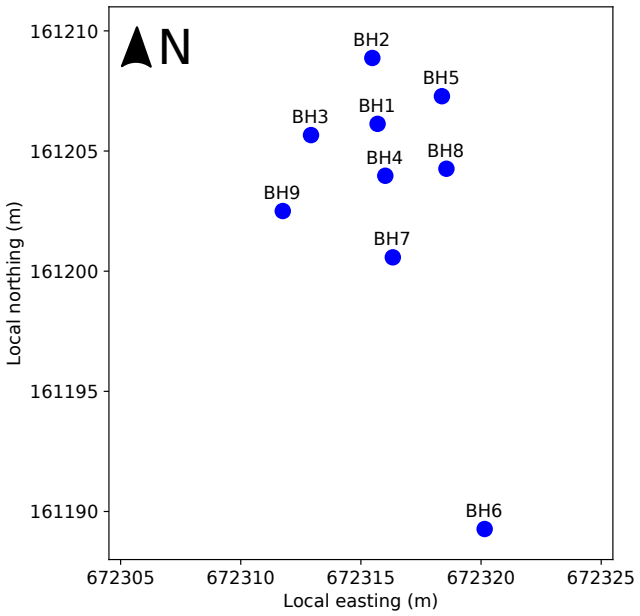

Fig. 1. Map of the surface locations of the boreholes (BH1 - BH9) that were drilled in the field campaign in 2018.

Seismometer Array in 2017

The seismometer array consists out of eight Lennartz 3D 1s seismometers deployed at the glacier surface with Omnirecs Data Cube digitizers sampling at 400 Hz and Nanometrics Centaur digitizers sampling at 500 Hz. A map with the station locations is shown in Fig. 2.

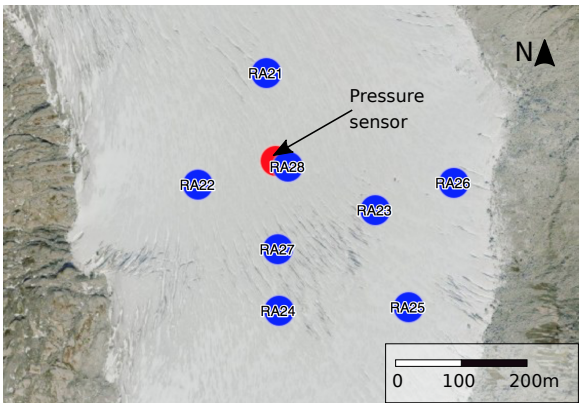

Fig. 2. Situational map of the instrumentation in 2017 showing the seismometer array deployed simultaneously with the pressure sensor.

EVENTS DIFFERENT FROM CRACK WAVES

Swarms of sound waves

In Fig. 3 we show further events form the pressure sensor data of 2017, but that are different from crack waves. We interpret these pressure spikes as non-dispersive sound waves.

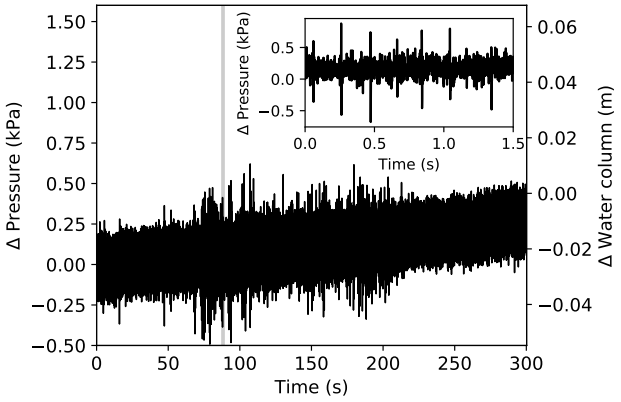

Fig. 3. Series of multiple impulsive sound waves. The inserted window is a zoom into the thin gray shaded time of the main plot. A regular inter-event time between the sound waves is apparent.

Pressure drop and oscillations

Figure 4 shows the 23 cm pressure drop that occurred one hour after the one that is presented in the paper. Some of the pressure oscillations after the pressure drop have a comparable waveform to the crack waves that are taken into account for the ensemble analysis. However, in some aspects, such as decay behavior and spectral content, many differ from what is expected for crack waves.

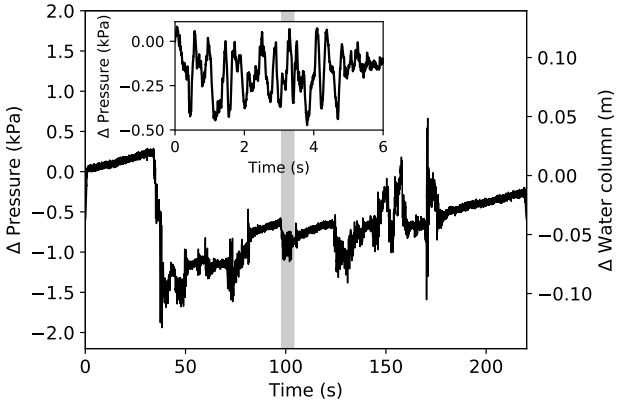

Fig. 4. 23 cm pressure drop accompanied by multiple pressure oscillation. The inserted window is a a zoom into the gray shaded time of the main plot.

CRACK WAVE TIMES

From the visual scan of the 2017 pressure sensor data, we use events at the following times for the crack wave analysis together with their approximate duration and the Q factor estimated by counting full oscillation cycles of the dominant frequency. The raw data of the crack wave events can be found in the sub-directory "2017events/data/" of the file 2017event.zip within this supplementary material.

Table 1. Crack wave times with their approximate duration and the quality factor Q from counting oscillations of the dominant frequency.

Time (UTC)	Duration	Q
2017-08-21 16:12:00.15	2.2	6
2017-08-21 16:18:32.7	1.35	6
2017-08-21 16:18:36.25	2.0	8
2017-08-21 16:18:39.0	3.0	12
2017-08-21 16:18:42.3	0.85	3
2017-08-21 16:18:43.5	1.6	10
2017-08-21 16:18:45.65	1.2	5
2017-08-21 16:18:46.95	1.6	6
2017-08-21 16:18:49.5	2.05	6
2017-08-21 16:18:52.0	1.7	7
2017-08-21 16:18:53.85	1.75	5
2017-08-21 16:18:58.4	2.4	10
2017-08-21 16:19:09.75	3.05	11
2017-08-21 16:19:21.35	1.5	7
2017-08-21 16:19:32.65	2.0	9
2017-08-21 17:11:20.2	1.15	7
2017-08-22 10:09:29.0	57.0	65
2017-08-22 10:13:29.5	90.5	110
2017-08-22 10:16:06.55	2.85	11
2017-08-22 10:16:13.15	2.05	9
2017-08-22 10:16:19.15	1.0	7
2017-08-22 10:16:24.85	4.7	14
2017-08-22 10:18:39.0	71.0	70
2017-08-22 10:22:30.0	80.0	80
2017-08-22 10:27:43.0	67.0	70

DETAILED DATA ANALYSIS

Our crack waves show a swarming behavior. For the impulsive ones in particular this means that directly after one crack wave decayed, a new onset can happen. Thus we have to set the window for the calculation of the spectral content tight around the event, which affects the frequency resolution.
Here we describe the procedure that we used for the quantitative analysis of the crack wave frequency spectra. In the html file "crack_wave_analysis.html" this analysis can be retraced:

1. We plot the waveform of the crack wave and check the window alignment (Fig. 5).

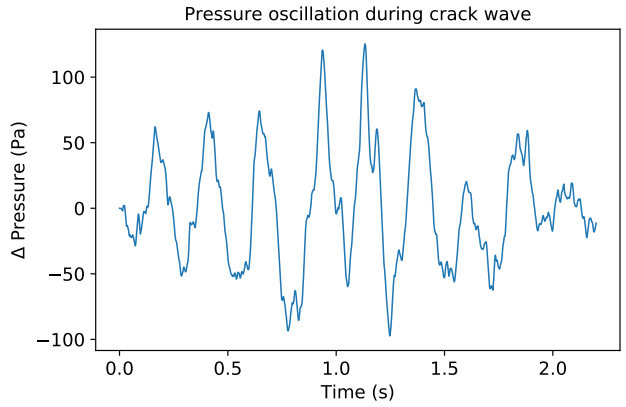

Fig. 5. Waveform of one impulsive crack wave.

2. For each crack wave we calculate its spectrum (Fig. 6).

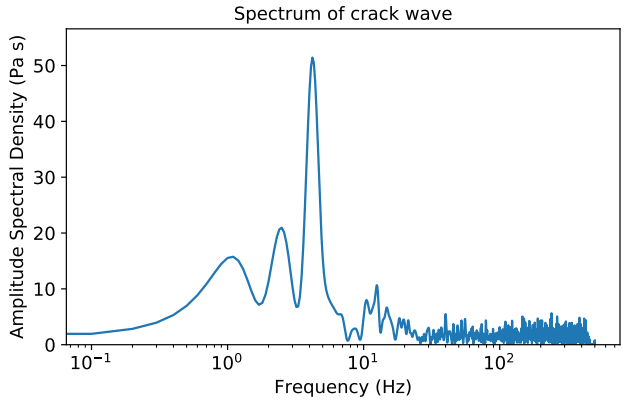

Fig. 6. Representative spectrum of one impulsive crack wave. (logarithmic frequency scale)

3. To each spectrum we apply a peak detection and fit gaussians to each detected peak (Fig. 7).

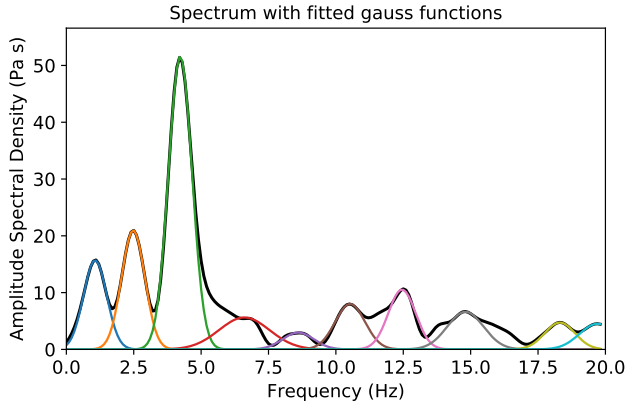

Fig. 7. Representative spectrum (black line) of one impulsive crack wave with gaussians fitted to the peaks (various colors). We only take frequencies below 20 Hz into account.

4. From the gauss fits we retrieve peak positions and the corresponding peak widths (Tab. 2).

Table 2. Spectral peaks and their widths.

Frequency (Hz)	Frequency width (Hz)
1.07	0.72
2.48	0.72
4.23	0.73
6.60	1.56
8.60	0.96
...	...

5. We condense all the detected peaks of all crack waves with their corresponding peak widths into one list (not shown here).
6. We apply a kernel density estimation (KDE) on the distribution of the peak positions (Fig. 8).

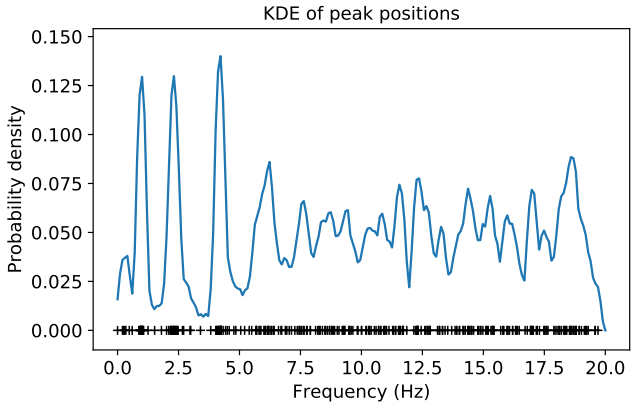

Fig. 8. Kernel density estimation of the distribution of peaks from all crack wave events. Every black marker represents the peak position of a single detected spectral peak.

7. We apply a peak detection to the output of the KDE and fit gaussians to each detected peak (Fig. 9)

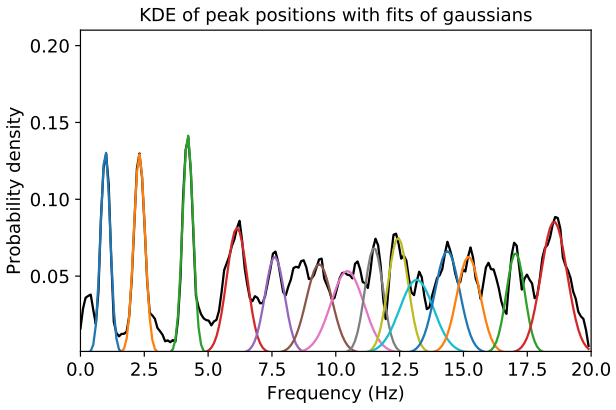

Fig. 9. Kernel density estimation (black line) of the distribution of peaks from all crack wave events with gaussians fitted to the peaks (various colors).

8. From the fitted gaussians, we obtain the center frequencies, with the highest peak density and their relative spreading given by the width of the gaussians (Tab. 3):

Table 3. Peaks in the KDE and their widths.

Frequency (Hz)	Sigma (Hz)	Probability Density
0.98	0.19	0.13
2.31	0.22	0.13
4.20	0.20	0.14
6.13	0.40	0.08
7.61	0.38	0.06
9.35	0.50	0.06
...	...	..

9. We set the width of the gaussians of each peak in the KDE to be the range within which spectral peaks will be associated with one frequency peak. From the ensemble of spectral peaks within this range, we calculate the mean of the spectral peak position and width (Tab. 4). This leads to the final overtone estimation together with the overtone width.

Table 4. Final estimation of spectral peak position and width.

Mean (Hz)	Mean Std. (Hz)	Width (Hz)	Width Std. (Hz)
0.98	0.05	0.64	0.17
2.30	0.11	0.77	0.26
4.18	0.08	0.87	0.19
6.14	0.19	0.92	0.18
7.61	0.19	0.60	0.26
9.32	0.27	0.88	0.30
...	...	...	...

Water layer patch size from overtones

The water patch sizes estimated from the overtones are listed in Tab. 5.

Table 5. Water layer patch size calculated as the mean between the pure ice and pure rock fracture for all overtones.

Peak Frequency	Q	Q Std.	Length (m)	Length Std. (m)	Aperture (mm)	Aperture Std. (mm)
1.0	1.5	0.4	19.8	1.8	1.1	0.3
2.3	3.0	1.0	12.1	1.4	1.5	0.5
4.2	4.8	1.1	8.6	0.7	1.7	0.4
6.1	6.6	1.3	7.0	0.5	2.0	0.4
7.6	12.6	5.4	7.2	1.0	3.4	1.4
...	...	...	...	...	...	...

Output data

The complete output data of the analysis can be found in the sub-directory "2017events/analysis/" of the file 2017event.zip within this supplementary material. It has following sub-directories:

spectra/ contains waveforms, spectra, and spectral peak fits of every single crack wave we used for the analysis and are named with the crack wave event time in the format "yyyy-MM-dd-HH-mm-ss".

kde/ contains a plot of the KDE of the peak positions, and a plot of the gauss fits to them, as well as the fitting parameters of the gaussians.

final/ contains the file final_peaks.csv with the estimated peak positions. The files final_values.csv, final_values_rock.csv, and final_values_ice.csv contain the calculated geometrical extensions calculated as the mean for combined rock and ice walls, respectively for each rock and ice separately.

BASAL CONDITIONS

The basal conditions at the bed of Rhonegletscher are visible in the freshly deglaciated area (see Fig. 10). Undulations of the bedrock on the order of 5 m to 10 m exist with till filled patches in between.

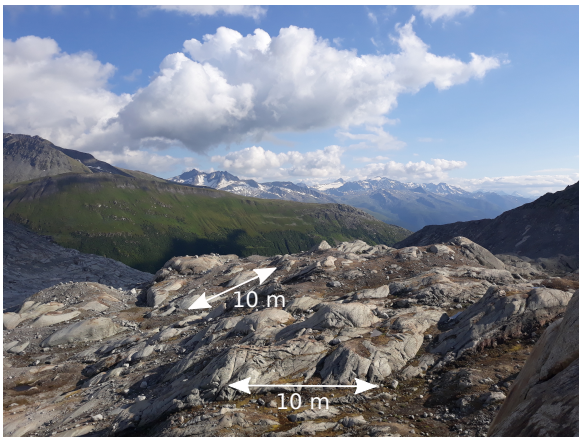

Fig. 10. De-glaciated area of Rhonegletscher. White arrows roughly indicate dimensions.

Borehole footage 2017

Fig. 11 shows a close footage of the granite bedrock, taken with the borehole camera at the location of the pressure sensor in 2017. The camera was about 10 cm above the bedrock. Scratches aligned with the glacier flow are visible. The confirm that there exists a hard bedrock at the site of the pressure sensor measurements.

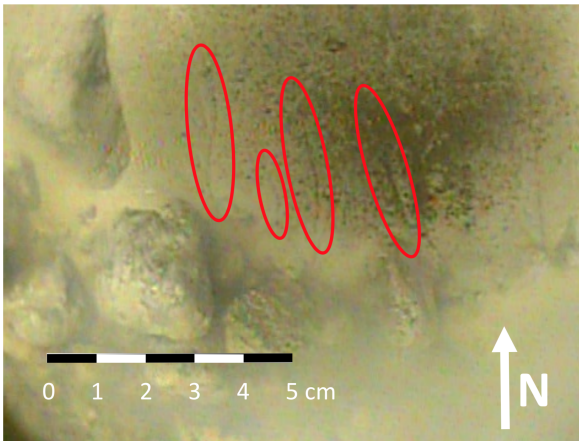

Fig. 11. Scratches in the hard granite bedrock in the borehole from 2017.

Borehole footage 2018

The video in the file "dynamic_till_2018.avi" of this supplementary material is a time lapse of the glacier bed in borehole 2 at the drilling site in summer 2018. It is located in 2.5 m distance from the location where we recorded crack waves with a pressure sensor. The timespan of the time laps is about 3.5 hours. The video shows that the two small rocks are pushed upwards (towards the borehole camera) by the fine silt material. During this period the hydrostatic pressure in all surrounding boreholes was increasing.